Journal of Materials Chemistry C

PAPER

View Article Online
View Journal | View Issue

Cite this: J. Mater. Chem. C, 2015, 3, 2479

Fluorene co-polymers with high efficiency deep-blue electroluminescence†

José Santos,[a] Javan H. Cook,[b] Hameed A. Al-Attar,[b] Andrew P. Monkman*[b] and Martin R. Bryce*[a]

Received 2nd December 2014
Accepted 25th January 2015

DOI: 10.1039/c4tc02766c

www.rsc.org/MaterialsC

Two new deep blue emitting co-polymers are synthesised and exploited in highly-efficient solution-processed polymer light-emitting diodes (PLEDs). A key molecular design feature is selective functionalisation of 9,9-diphenylfluorene to disrupt backbone π-conjugation, thereby promoting luminescence from short emissive domains (λ_{max}^{EL} 422 and 401 nm for **P1** and **P2** devices, respectively). PLEDs using **P1** and **P2** in the hybrid architecture ITO/PEDOT:PSS/polymer/TPBi/LiF/Al show low turn-on voltages and remarkably high EQE values of $\eta_{ext,max}$ 3.3%, L_{max} of 167 cd m^{-2} with CIE$_{xy}$ coordinates (0.17, 0.10) for **P1**; and 3.9%, 274 cd m^{-2}, CIE$_{xy}$ (0.17, 0.07) for **P2**. These performances are currently among the best for PLEDs with CIE$_y \leq 0.10$.

Introduction

Since organic materials were first exploited in organic light emitting diodes (OLEDs),[1,2] they have experienced a rapid process of research and development, which has culminated in recent years in a number of commercial applications in displays and solid-state lighting.[3] Compared to other technologies, OLEDs allow reduced power consumption, faster response times, larger viewing angles, smaller sizes and greater ranges of colour and contrast.[4–6] A main advantage of OLEDs, especially polymeric systems, is that their solubility allows rapid industrial-scale device fabrication by solution processing techniques such as spin-coating, roll-to-roll processing and ink-jet printing.[7]

Embedding an inorganic dopant into an organic host has been a very successful strategy to achieve internal quantum efficiencies close to 100% in phosphorescent OLEDs (PhOLEDs) giving devices with external quantum efficiency (EQE) yields of up to *ca.* 20% for red, green and sky blue PhOLEDs.[8] However, this approach faces several limitations related to the scarcity and high costs of the dopants (typically Ir, Pt complexes) and, more specifically, the lack of emitters with good blue colour coordinates, long-life stability and compatible host materials. Obtaining efficient deep blue PhOLEDs (with emission below 450 nm) has, therefore, proved to be elusive.[9]

As an alternative strategy, pure-fluorescent small-molecule organic emitters have yielded deep blue OLEDs with EQEs of 3–6%.[10] However, efficient deep blue *polymeric* devices (PLEDs) with the added advantage of solution processability are very rare.[11] A major challenge for the rational design of such systems is that for blue emission the electronic conjugation along the polymer chain must be confined to short segments, but without completely destroying the polymer's charge carrier transport capabilities. In previous work, we[12,13] and others[14] have attached bulky side chains to induce a twist into the polymer backbone and thereby isolate minimal conjugated segments. Nevertheless, in order to push the emission further into the blue (below λ_{max} 450 nm) alternative strategies are required.

In this work we designed polymers with short conjugated segments which are separated by 9,9-diphenylfluorene moieties, as shown in Fig. 1. Having small conjugated segments is pivotal in order to obtain deep blue emission; nevertheless, retaining some conjugation is essential as stated earlier to keep the charge transport properties. The novelty in the present work is the use of 9,9-diphenylfluorene as a conjugation disrupter unit in our new fluorene-based polymers in order to confine the minimal conjugated domains necessary for deep blue emission. This moiety disrupts the conjugation between the fluorene core and the phenyl rings due to its sp^3 hybridised C(9) carbon. In **P1**, which is a regiorandom co-polymer, the minimal conjugated domain is localised over the main chain and consists of 2,7-linked 9,9-dihexylfluorene units linked to 9,9-diphenylfluorene (in a 70 : 30 ratio) by the phenyl rings. In **P2** the minimal conjugated part is isolated from the polymer main chain as pendant groups, consisting of two *N*-linked 3,6-di-*tert*-butylcarbazole units attached to 9,9-diphenylfluorene at its 2 and 7 positions. The photophysics of the co-polymers is reported. They function as deep blue fluorescent emitters in PLEDs, whose performances are currently among the best for PLEDs with CIE$_y \leq 0.10$.

[a]Department of Chemistry, Durham University, Durham, DH1 3LE, UK
[b]Department of Physics, Durham University, Durham, DH1 3LE, UK

† Electronic supplementary information (ESI) available: Synthesis and characterisation of monomer **4**; absorption spectra of **P1** and **P2**; CIE diagrams and a photograph of a **P1** device. See DOI: 10.1039/c4tc02766c

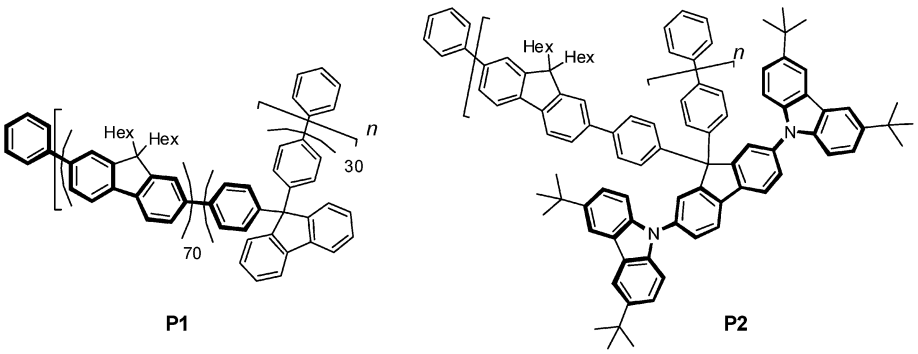

Fig. 1 Structures of the new deep blue emitting co-polymers studied in this work. The minimal conjugated domains are highlighted in bold. The 70 : 30 ratio of units in **P1** is based on the monomer feed ratio; the units are regiorandomly distributed.

Results and discussion

Polymer synthesis

The synthesis of polymers **P1** and **P2** was carried out under standard Suzuki–Miyaura copolymerization conditions[15] as shown in Scheme 1 and described in detail in the ESI.† To obtain **P2** we developed the novel building-block **4** consisting of two carbazole units *N*-bonded to positions 2 and 7 of 9,9-di(4-bromophenyl)fluorene (Scheme S1, ESI†). This co-monomer was synthesised from 9,9-di(4-bromophenyl)-2,7-diiodofluorene, which is, again, a new and versatile reagent bearing two different functionalisations allowing a wide variety of chemical transformations. The co-polymers were characterised by GPC-UV-vis data using polystyrene standards: **P1** M_w 49 655 Da, M_n 13 949 Da; **P2** M_w 60 252 Da, M_n 24 737 Da.

Optical properties

The spectroscopic data for polymers **P1** and **P2** is summarised in Table 1. Their absorption spectra are shown in the ESI† and their photoluminescence spectra are shown in Fig. 2. The polymers are deep blue emitters (λ_{max}^{PL} in thin films: 427 and 425 nm, respectively). They exhibit very little solvatochromism and the small differences observed can be attributed to a change in refractive index between the solvents, as observed previously for blue fluorescent polymers.[12,13]

Table 1 Photophysical data for the polymers **P1** and **P2**

Polymer	Solvent/film	λ_{max}^{abs}/nm	λ_{max}^{PL}/nm	PLQY, Φ_{PL} [a]	E_T^{onset} [b]/eV
P1	Ethyl acetate	363	412		
	Cyclohexane	360	412		
	Film	375	427	0.44	2.38
P2	Ethyl acetate	344	394		
	Cyclohexane	344	392		
	Film	367	425	0.52	2.38

[a] PLQY is the photoluminescence quantum yield. [b] E_T is the triplet energy.

From the emission data in Table 1 it can be seen that the additional two carbazole units in **P2**, and the steric bulk associated with them, causes a substantial blue shift of 15–20 nm in solution compared to **P1**, and a reduced blue shift in thin films. This blue shift can be ascribed to the slightly reduced π-conjugation length in **P2** compared to **P1**. The addition of the carbazole units also introduces a new peak in the solution PL spectra. This is especially observed in cyclohexane (Fig. 1, panel b) where there is a well-resolved additional peak at 371 nm which corresponds to emission spectra reported previously for small-molecule carbazole chromophores.[16]

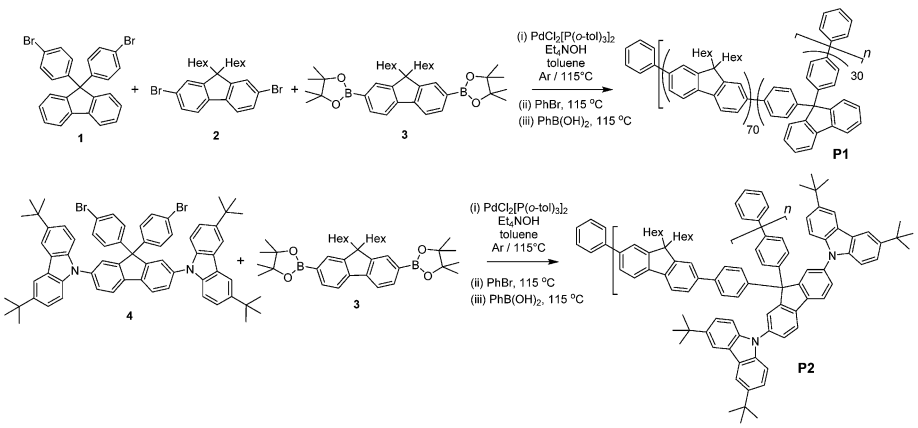

Scheme 1

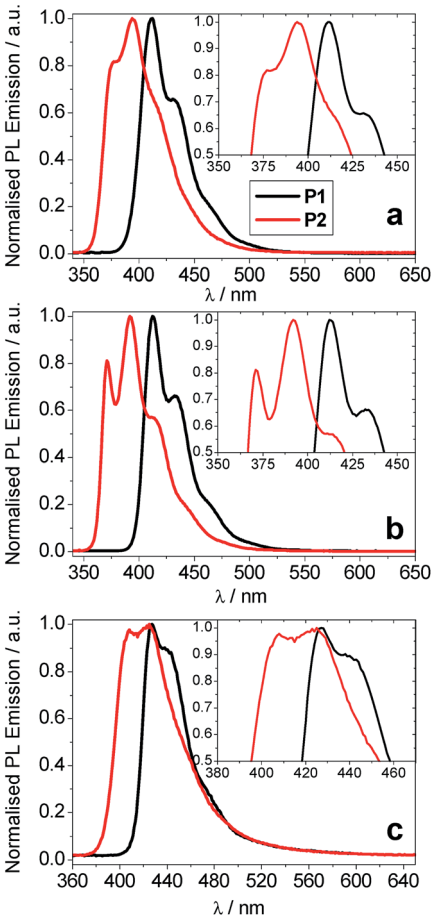

Fig. 2 Normalised PL emission spectra for polymers **P1** and **P2** (a) in ethyl acetate; (b) in cyclohexane; (c) in thin film. The insets show a magnification of the λ_{max} region.

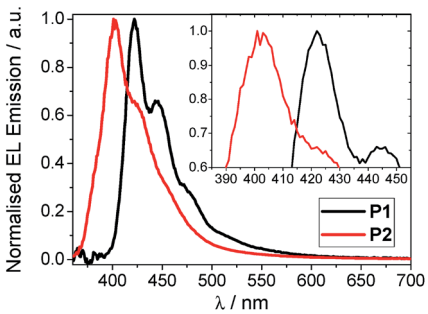

Fig. 3 Normalised EL emission spectra for polymers **P1** and **P2**. Inset shows a magnification of the λ_{max} region. The device structure is stated in Table 2, footnote *a*.

The film PLQY values for polymers **P1** and **P2** are similar, with values of Φ_{PL} 0.44 and 0.52, respectively. The observed triplet levels for **P1** and **P2** (E_T^{onset} 2.38 eV) are consistent with data for the polymers with restricted π-conjugation investigated previously.[12,13,17,18]

Deep blue PLED device fabrication and properties

Hybrid devices were fabricated for polymers **P1** and **P2** using the structure: glass|ITO (150 nm)|PEDOT:PSS 1.5 (70 nm)|LEP (**P1** 70 nm, **P2** 30 nm)|TPBi (20 nm)|LiF (1 nm)|Al (100 nm). For all of the devices, no other dopants or transporters were added to the light emitting polymer (LEP) layer. The thicknesses of the two LEP layers were determined after prior thickness optimisation for device performance. 1,3,5-Tris(*N*-phenylbenzimidazole-2-yl)benzene (TPBi) is a standard electron-injecting layer to improve device performance (increased efficiency and brightness, and reduced turn-on voltage).[19]

Both polymers display remarkably deep blue EL emission (Fig. 3). In the case of **P1** the EL peaks at 422 nm with a shoulder at 440 nm, whilst for **P2** the emission is even deeper blue, peaking at 401 nm with a small shoulder at 424 nm. This difference between **P1** and **P2** is a consequence of **P2**'s reduced π-conjugation length.

The device results are shown in Table 2 and Fig. 4. **P1** devices have maximum EQE of 3.3% with $CIE_{x,y}$ coordinates [turn on (0.16, 0.07) and peak (0.17, 0.10)]. **P2** devices display extremely deep blue emission with a higher EQE (3.9%) and outstanding $CIE_{x,y}$ coordinates [turn on (0.16, 0.06) and peak (0.17, 0.07)]. CIE diagrams are shown in the ESI.†

The addition of the carbazole substituents to the pendant group in **P2** has the desirable effect of increasing the current density passing through the device, the maximum brightness and the maximum EQE. We have recently shown that breaking the conjugation of a polymer typically reduces its conductivity resulting in limited maximum brightness.[13] However, this effect seems to have been overcome in **P2** by the intrinsic conduction properties of the carbazole groups, causing the current density to double with respect to **P1** and the maximum brightness to increase from 167 (**P1**) to 274 cd m^{-2} (**P2**). The increase in EQE (maximum 3.3% for **P1** and 3.9% for **P2**) is most likely due to an increase in hole mobility imparted by the carbazole units.[20] This would result in a more balanced proportion of carriers recombining in the light-emitting polymer layer, reducing the amount of wasted carriers reaching the electrodes. The decrease in current efficiency from **P1** to **P2** is expected, despite the reverse

Table 2 Electroluminescent device data[a]

	V_{on}[b]/V	Brt/cd m^{-2}	EQE/%	Dev eff/cd A^{-1}	Brt_{max}/cd m^{-2}	EQE_{max}/%	Dev eff_{max}/cd A^{-1}	Lum_{max}/lm W^{-1}	CIE (*x*,*y*)[d]	CIE (*x*,*y*)[e]
P1	3.75	92[c]	1.55[c]	0.90[c]	167	3.3	1.6	1.39	0.16, 0.07	0.17, 0.10
P2	4.25	63[c]	2.10[c]	0.65[c]	274	3.9	1.3	0.99	0.16, 0.06	0.17, 0.07

[a] Device architecture: ITO/PEDOT:PSS/polymer/TPBi/LiF/Al. [b] V_{on} is the turn-on voltage, defined here as the voltage at which the device reaches a brightness of 10 cd m^{-2}. [c] A comparison current density of 10 mA cm^{-2} was selected. [d] CIE coordinates at the turn-on voltage (10 cd m^{-2}). [e] CIE coordinates at the maximum brightness. CIE diagrams are shown in the ESI.

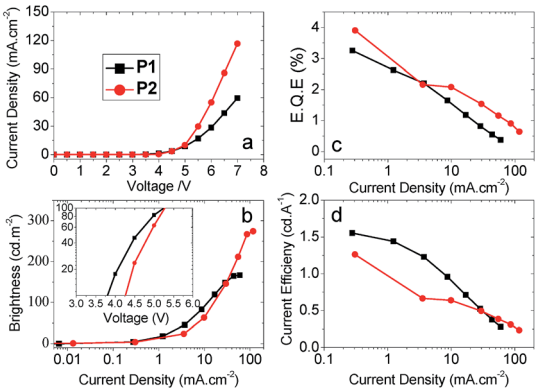

Fig. 4 Plots of (a) *J*–*V* curves. (b) Luminance *vs.* *J*. (c) EQE *vs.* *J*. (d) Device efficiency *vs.* *J* for the polymers **P1** and **P2**. Inset to (b) shows the low turn-on voltages for the two devices in a plot of luminance *vs.* V. The device structure is stated in Table 2, footnote *a*.

trend in EQE, as this value depends on the luminosity function and **P2** produces a deeper blue emission than **P1**.

Conclusions

New polyfluorene based co-polymers have been synthesised incorporating 9,9-diphenylfluorene to restrict the π-conjugation to short segments. For **P1** the minimal conjugated domain is in the main chain whereas for **P2** the minimal structure is a carbazole–fluorene segment isolated from the polymer main chain as a pendant unit. For **P1** deep blue emission peaks at *ca.* 422 nm with $CIE_{x,y}$ (0.17, 0.10) with a maximum EQE of 3.3% and brightness of 167 cd m^{-2}. For **P2**, the efficiency reaches 3.9% EQE, with a maximum brightness of 274 cd m^{-2} and very deep blue emission peaking at *ca.* 401 nm with $CIE_{x,y}$ (0.17, 0.07). The PLEDs, which have a simple device architecture, turn on at low voltages (3.75 and 4.25 V, respectively, for **P1** and **P2**) and have good colour stability. Their performance is currently among the best for PLEDs with $CIE_y \leq 0.10$, representing a significant contribution to the field and fulfilling the requirements for full-colour displays.

Experimental section

Synthesis of polymers P1 and P2

General Suzuki copolymerization procedure. Monomers **1**,[21] **2**[22] and **3**[23] were synthesised as reported in the literature. The synthesis of monomer **4** is described in the SI. All monomers were dissolved in dry toluene (7 mL) and degassed by bubbling argon into the solution for 30 min [in the case of **P1** (200 mg, 0.341 mmol) of boronic ester **3** were used, along with (97 mg, 0.205 mmol) and (67 mg, 0.136 mmol) of halogenated derivatives **1** and **2**, respectively; for polymer **P2** (200 mg, 0.341 mmol) of **3** and (352 mg, 0.341 mmol) of **4** were used]. $PdCl_2[P(o\text{-tol})_3]_2$ (1% mol) was then added and the reaction degassed for an additional 15 min. A degassed aqueous Et_4NOH solution (4 mL, 20% w/w) was added and the reaction mixture was stirred at 115 °C for 24 h. All co-polymers were end-capped with phenyl units by addition of bromobenzene (1 mL), followed 1 h later by benzeneboronic acid (100 mg). The reaction mixture was cooled and poured into methanol (300 mL). The resulting precipitate was filtered and sequentially washed with methanol, water and methanol. After drying, the solid was redissolved in chloroform (20 mL) and a solution of palladium scavenger (1 g of sodium diethyldithiocarbamate trihydrate) in water (20 mL) was added. The mixture was then stirred overnight at 60 °C. The organic layer was separated and sequentially washed with dilute HCl (5%), concentrated sodium acetate and water. The resulting organic extracts were filtered through a plug of celite and concentrated under vacuum. The concentrate was added dropwise to methanol to precipitate the co-polymers which were isolated as white solids and characterised by GPC-UV-vis using polystyrene standards.

Optical characterisation. Absorption spectra for solution and solid state sample were obtained using a Shimadzu UV-vis-NIR spectrophotometer whilst emission spectra were acquired using a Jobin-Yvon fluoromax spectrofluorimeter. The excitation wavelengths were determined from the maximum absorbance of the polymers as obtained from the absorption spectra. The triplet energies of solid state samples at 16 K were obtained using a gated luminescent measurement of the phosphorescence.[24] Solutions were prepared in ethyl acetate or cyclohexane, and the OD kept below 1.0. Solid state samples were drop-cast from a 1 : 1 mixture of 175 mg mL^{-1} zeonex and 0.5 mg mL^{-1} of the polymer, both in chlorobenzene, and had a maximum absorbance of 2.0 OD.

Device fabrication and characterisation

The devices comprised an ITO anode (150 nm, 16 Ω $square^{-1}$) commercially pre-coated on a glass substrate (24 mm × 24 mm). The substrates were cleaned sequentially with acetone, isopropanol and acetone in a sonic bath for a period of 9 min each. They were then exposed to low pressure plasma for a period of 3 min and treated with UV-ozone for a further 4 min. A hole-injection layer (HIL) of PEDOT:PSS of thickness 70 nm was deposited by spin coating and then baked on a hotplate at 200 °C for 3 min to remove any residual moisture. The PEDOT:PSS used was the commercially available HIL 1.5 from Heraeus Precious Metals, Germany. Active layers of polymers **P1** and **P2** were prepared in a solution of chlorobenzene with the concentration varied to produce devices of optimal thickness, and then spun on top of the PEDOT:PSS. The device was then annealed at 120 °C on a hotplate for 10 min to remove residual chlorobenzene. An electron injection layer (EIL) consisting of a 20 nm layer of 1,3,5-tris(*N*-phenylbenzimidazol-2-yl)benzene (TPBi) was thermally evaporated directly on top of the polymer layer. This was followed by a 1 nm thick lithium fluoride (LiF) cathode, which was thermally evaporated using a shadow mask to produce parallel strips perpendicular to the ITO anodes, forming four individually addressable pixels per substrate, each of area 5 mm × 4 mm. The LiF was capped with a 100 nm thick layer of aluminium to protect it from oxidation. An evaporation pressure of *ca.* 10^{-6} mbar and a rate of *ca.* 0.1 nm s^{-1} were used for all of evaporated layers. The devices were then encapsulated

with DELO UV curable epoxy (Katiobond) and a 12 × 12 mm glass cover slide. The devices were characterised in a calibrated Labsphere LMS-100 integrating sphere, connected to a USB 4000 CCD spectrometer supplied by a 30 μm UV-vis fibre optic cable, under steady state conditions. Layer thicknesses were measured using a J. A. Woolam VASE Ellipsometer after having been spin coated onto Si/SiO_2 substrates. The non-uniformity of the organic layer thicknesses across the samples leads to a 5–10% error in device efficiencies and all measurements were averages over at least four devices.

Acknowledgements

The authors acknowledge the financial support of the Durham Energy Institute and EPSRC.

References

1 C. W. Tang and S. Van Slyke, *Appl. Phys. Lett.*, 1987, **51**, 913–915.
2 J. H. Burroughes, D. D. C. Bradley, A. R. Brown, R. N. Marks, K. Mackay, R. H. Friend, P. L. Burn and A. B. Holmes, *Nature*, 1990, **347**, 539–541.
3 (*a*) *Organic Light Emitting Devices: Synthesis, Properties and Applications*, ed. K. Mullen and U. Scherf, Wiley-VCH, Weinheim, 2006; (*b*) Z. Li and H. Meng, *Organic Light-Emitting Materials and Devices*, CRC, Boca Raton, FL, 2006; (*c*) K. L. Chan, R. E. Martin, P. G. Jokisz and A. B. Holmes, *Chem. Rev.*, 2009, **109**, 897–1091; (*d*) C. Rothe, *Laser Photonics Rev.*, 2007, **1**, 303–306; (*e*) N. T. Kalyani and S. J. Dhoble, *Renewable Sustainable Energy Rev.*, 2012, **16**, 2696–2723; (*f*) H. Sasabe and J. Kido, *Chem. Mater.*, 2011, **23**, 621–630; (*g*) P. L. Burn, S. C. Lo and I. D. W. Samuel, *Adv. Mater.*, 2007, **19**, 1675–1688; (*h*) K. T. Kamtekar, A. P. Monkman and M. R. Bryce, *Adv. Mater.*, 2010, **22**, 572–582; (*i*) L. Ying, C.-L. Ho, H. Wu, Y. Cao and W.-Y. Wong, *Adv. Mater.*, 2014, **26**, 2459–2473; (*j*) R. Mertens, *The OLED handbook. A Guide to OLED Technology, Industry and Market*, 2014, www.oled-info.com/handbook.
4 S. C. Stinson, *Chem. Eng. News*, 2000, **78**, 22–23.
5 W. E. Howard, *Sci. Am.*, 2004, **290**, 76–81.
6 R. Friend, J. Burroughes and T. Shimoda, *Phys. World*, 1999, **12**, 35–40.
7 A. C. Arias, J. D. MacKenzie, I. McCulloch, J. Rivnay and A. Salleo, *Chem. Rev.*, 2010, **110**, 3–24.
8 (*a*) C. Ulbricht, B. Beyer, C. Friebe, A. Winter and U. S. Schubert, *Adv. Mater.*, 2009, **21**, 4418–4441; (*b*) K. Chao, K. Shao, T. Peng, D. Zhu, Y. Wang, Y. Liu, Z. Su and M. R. Bryce, *J. Mater. Chem. C*, 2013, **1**, 6800–6806.
9 (*a*) S. Lee, S.-O. Kim, H. Shin, H.-J. Yun, K. Yang, S.-K. Kwon, J.-J. Kim and Y.-H. Kim, *J. Am. Chem. Soc.*, 2013, **135**, 14321–14328; (*b*) C.-H. Yang, M. Mauro, F. Polo, S. Watanabe, I. Muenster, R. Frohlich and L. de Cola, *Chem. Mater.*, 2012, **24**, 3684–3695.
10 (*a*) Y. Yang, P. Cohn, S.-H. Eom, K. A. Abboud, R. K. Castellano and J. Xue, *J. Mater. Chem. C*, 2013, **1**, 2867–2874; (*b*) J. Ye, Z. Chen, M.-K. Fung, C. Zheng, X. Ou, X. Zhang, Y. Yuan and C.-S. Lee, *Chem. Mater.*, 2013, **25**, 2630–2637; (*c*) M. Zhu and C. Yang, *Chem. Soc. Rev.*, 2013, **42**, 4963–4976.
11 U. Giovanella, C. Botta, F. Galeotti, B. Vercelli, S. Battiato and M. Pasinbi, *J. Mater. Chem. C*, 2013, **1**, 5322–5329.
12 K. T. Kamtekar, H. L. Vaughan, B. P. Lyons, A. P. Monkman, S. U. Pandya and M. R. Bryce, *Macromolecules*, 2010, **43**, 4481–4488.
13 J. H. Cook, J. Santos, H. Li, H. A. Al-Attar, M. R. Bryce and A. P. Monkman, *J. Mater. Chem. C*, 2014, **2**, 5587–5592.
14 J. Liu, S. Hu, W. Zhao, Q. Zou, W. Luo, W. Yang, J. Peng and Y. Cao, *Macromol. Rapid Commun.*, 2010, **31**, 496–501.
15 (*a*) J. Murage, J. W. Eddy, J. R. Zimbalist, T. B. McIntyre, Z. R. Wagner and F. E. Goodson, *Macromolecules*, 2008, **41**, 7330–7338; (*b*) J. Sakamoto, M. Rehahn, G. Wegner and A. D. Schluter, *Macromol. Rapid Commun.*, 2009, **30**, 653–687.
16 D. Shoucheng, L. Zhen and Q. Jingui, *J. Phys. Chem. B*, 2009, **113**, 434–441.
17 K. Brunner, A. van Dijken, H. Börner, J. J. A. M. Bastiaansen, N. M. M. Kiggen and B. M. W. Langeveld, *J. Am. Chem. Soc.*, 2004, **126**, 6035–6042.
18 B. Chen, L. Yu, B. Liu, J. Feng, Z. Liu, L. Ying, Y. Li and W. Yang, *J. Polym. Sci., Part A: Polym. Chem.*, 2014, **52**, 1037–1046.
19 J.-H. Jou, W.-B. Wang, S.-M. Shen, S. Kumar, I.-M. Lai, J.-J. Shyue, S. Lengvinaite, R. Zostautiene, J. V. Grazulevivius, S. Grigalevicius, S.-Z. Chen and C.-C. Wu, *J. Mater. Chem.*, 2011, **21**, 9546–9552.
20 (*a*) K. Brunner, A. van Dijken, H. Borner, J. J. A. M. Bastiaansen, N. M. M. Kiggen and B. M. W. Langeveld, *J. Am. Chem. Soc.*, 2004, **126**, 6035–6042; (*b*) P.-L. T. Boudrealt, S. Beaupre and M. Leclerc, *Polym. Chem.*, 2010, **1**, 127–136; (*c*) H. Yi, S. Al-Faifi, A. Iraqi, D. C. Watters, J. Kingsley and D. G. Lidzey, *J. Mater. Chem.*, 2011, **21**, 13649–13656.
21 D. Yu, Y. Zhao, H. Xu, C. Han, D. Ma, Z. Deng, S. Gao and P. Yan, *Chem.–Eur. J.*, 2011, **17**, 2592–2596.
22 T.-C. Lin, C.-Y. Liu, B.-R. Huang, J.-H. Lin, Y.-K. Shen and C.-Y. Wu, *Eur. J. Org. Chem.*, 2013, 498–508.
23 S. P. Dudek, M. Pouderoijen, R. Abbel, A. P. H. J. Schenning and E. W. Meijer, *J. Am. Chem. Soc.*, 2005, **127**, 11763–11768.
24 (*a*) V. Jankus, C. Winscom and A. P. Monkman, *J. Chem. Phys.*, 2009, **130**, 074501; (*b*) C. Rothe and A. P. Monkman, *Phys. Rev. B: Condens. Matter*, 2003, **68**, 075208.